Article ID: 1671-3664(2006)02-0001-00

Identification and imaging of soil and soil-pile deformation in the presence of liquefaction

M. Zeghal[1†], P. V. Kallou[2‡], C. Oskay[3§], T. Abdoun[1†] and M. K. Sharp[4*]

1. *Dept. of Civ.and Env. Engrg.,RPI, Troy NY l2l80, USA*
2. *Mueser Rutledge Consulting Engineers, 225 W 34th Street, New York, NY 10122, USA*
3. *Dept. of Civ. and Env. Engrg., Vanderbilt University, Nashville, TN 37235, USA*
4. *Centrifuge Research & Development Center, Vicksburg, MS 39180, USA*

Abstract: A simple identification technique is developed to visualize the dynamic deformation mechanisms of centrifuge models of saturated soil and soil-pile systems using the measurements provided by sparsely distributed sensors. Cross-correlation analyses are employed first to assess the variation of shear wave velocity profile with time as soil experiences stiffness reduction and degradation during dynamic excitations. The corresponding time-dependent modal configurations are determined using the finite-element technique. These configurations are used along with recorded motions to evaluate optimal time histories of displacement and strain fields based on a spectral motion reconstruction. Visualizations of the response of infinite slope and soil-pile centrifuge models revealed salient and complex multi-dimensional deformation patterns, especially at high pore pressure ratios. The developed technique provides an effective tool to visualize and analyze the dynamic response of centrifuge, shake-table and field soil systems.

Keywords: pushover analysis; FEMA 356; infilled concrete frames; infill masonry panels; fiber-reinforced-polymer

1 Introduction

Soil and soil-structure systems exhibit complex response patterns during earthquake-induced liquefaction. These patterns depend on geotechnical properties, in-situ stress conditions and interaction with subsurface structural elements. Seismic records of full-scale systems during case histories provide a valuable source of information on the associated response mechanisms. However, the response of these systems is commonly monitored at sparsely distributed locations only, mostly because of technical and economic limitations. For instance, site field instrumentation generally consists of vertical (downhole) arrays of accelerometers and, in some cases, pore pressure sensors. Such arrays are adequate to analyze only the mechanisms of seismic amplification and liquefaction of free field sites when subjected to one-dimensional (vertical) seismic wave propagation (Elgamal *et al*., 2001; Zeghal *et al*., 1995). Thus, the multidimensional deformation characteristics and response mechanisms of complex soil and soil-structure systems during earthquakes have not been investigated thoroughly.

Dynamic testing of centrifuge or 1-g shake table physical models provides valuable complementary information to earthquake case histories. These tests generally furnish more comprehensive data sets than field instrumentations, especially in view of a new trend where soil systems are monitored using an increasing number of sensors (EERI, 2004). However, our ability to synthesize knowledge from measurements has not kept pace with our capability of collecting large set of experimental data. Simple interpretations of measurements, though useful, may not shed full light on the underlying phenomena. Investigation of the complex and multidimensional response of soil and soil-structure systems using these measurements necessitates more systematic tools, such as those provided by system identification and visualization techniques. In this regard, coupled identification and visualization analyses are gaining momentum in the field of geotechnical earthquake engineering (EERI, 2004; Vukazich and Mish, 1994). This momentum will eventually lead to an environment where physical modeling, computational simulations, system identification, and visualization tools are fully integrated to provide real time interpretation of data generated during testing.

Correspondence to: M. Zeghal, Dept. of Civ.and Env. Engrg.,RPI, Troy NY l2l80, USA
Tel: ; Fax:
E-mail: zeghal@rpi.edu
†Associate Professor; ‡Engineer; §Assistant Professor; *Director
Supported by: National Science Foundation Under Grant No. CMS-9984754
Received September 8, 2006; **Accepted** September 26, 2006

Herein, a simple identification technique is developed to visualize and analyze the dynamic displacement and deformation fields of soil and soil-pile systems using a limited number of measurements. This technique is based on a spectral motion reconstruction using modal shape functions. These functions are adaptively varied in time to account for stiffness reduction and degradation with strain amplitude and rise in pore pressure. An overview of liquefaction-induced deformation of soil systems is presented in the next section, followed by a description of the proposed technique, conducted analyses and obtained results.

2 Deformation and lateral-spreading of liquefied soils

Saturated cohesionless soil deposits experience increases in pore-fluid pressure, stiffness degradation and eventually liquefaction when subjected to moderate or strong seismic excitations. Such a softening leads to large permanent deformations and lateral spreading in the presence of a sloping ground or nearby free-front. The associated displacements typically range from several centimeters to few meters. Lateral spreading generally have damaging and costly effects on pile foundations, buried pipelines, port facilities and other civil systems. Severe destruction commonly occurs at the interface of liquefied and non-liquefied strata of multilayer sites, as demonstrated repeatedly by investigations following major earthquakes (Hamada *et al*., 1996; Tokimatsu, 1999).

The characteristics of liquefaction-induced deformation and lateral spreading depend on a number of factors. For instance, earthquake input motion features such as number of cycles, predominant frequency and peak acceleration were found to affect substantially the magnitude of spreading (Sharp, 1999; Kallou, 2002). Geotechnical soil properties also have an impact on the mechanisms of liquefaction and extent of lateral spreading. Dense soils exhibit a dilative response associated with instantaneous regains in stiffness at large strains. These soils may endure severe seismic excitations with relatively small lateral displacements. In contrast, saturated loose sandy soils experience large deformations and may undergo flow failures when subjected to dynamic loading (NRC, 1985).

Soil-systems exhibit essentially multidimendional lateral spreading and deformation patterns in the presence of structural elements or buried structures such as deep foundations or pipelines. These deformation patterns are still not fully understood, especially in view of the scarcity of in situ measurements. Centrifuge tests of small-scale physical models have emerged as an alternative source of information and a valuable tool to study the lateral spreading of soil and soil-structure systems during liquefaction (Dobry and Abdoun, 1998; Dobry and Abdoun, 2001). These tests rely on the use of laminar containers (Laak *et al*., 1994) which have flexible walls to allow large displacements along the lateral boundaries with supposedly minor normal reactions. More specifically, a laminar container consists of a stack of rectangular rings separated by linear roller bearings to permit relative movement between these rings in the direction of shaking with minimal friction.

3 Identification and imaging of soil system response

Identification and imaging techniques are valuable tools to comprehend the underlying mechanisms of complex physical phenomena, such as soil liquefaction, lateral spreading and soil structure interaction. Using these tools, researchers and engineers may synthesize and present information in ways that reveal the patterns, trends and relationships in experimental data. These data are commonly gathered at discrete locations, and interpolation is a fundamental step in the identification and imaging processes (Brodlie and Mashwama, 1997). Interpolation is a procedure whereby an empirical continuous model is constructed from a set of discrete measurements or recordings. Linear (local) interpolations are the simplest techniques to construct a data field using a dense set of experimental measurements (Brodlie and Mashwama, 1997; Perke 1995). Such interpolations have been used effectively along with measurements provided by downhole arrays of closely spaced accelerometers to analyze motion amplification and liquefaction of shallow strata of sites subjected to vertical seismic wave propagation. However, linear interpolations of response parameters of massive three-dimensional soil systems generally require a dense grid of measurements distributed over the whole system domain to achieve reasonably accurate empirical estimates. The smallest wavelength (or highest frequency) component of the interpolated parameters that can be recovered using such a grid is dictated by the Nyquist sampling theorem (Bendat and Piersol, 2000).

As mentioned above, the multidimensional dynamic response of soil systems is typically monitored using sparsely distributed sensors. Analyses of the displacement and deformation fields of a complex soil system, such as a soil-pile combination, based on sparse measurements require more sophisticated tools than simple local linear interpolations. For instance, employing higher order local interpolations to estimate these fields may lead to spurious spatial oscillations that are nothing but artifacts. The use of a limited number of measurements necessitates techniques capable of providing reasonable extrapolations in addition to accurate interpolations. Spectral motion reconstruction is shown below to fall within this context. This technique accounts for the physical characteristics and expected response patterns of a system under consideration to provide relatively accurate empirical approximations. This is especially true when the significant response of a geotechnical system is limited to a narrow band of low frequencies.

3.1 Spectral motion reconstruction

The dynamic displacement field, $\boldsymbol{u}(\boldsymbol{x}, t)$, of a soil system may be decomposed into permanent, $\boldsymbol{u}_{\mathrm{p}}$, and cyclic, $\boldsymbol{u}_{\mathrm{c}}$, components:

$$\boldsymbol{u}(\boldsymbol{x}, t) = \boldsymbol{u}(\boldsymbol{x}, t) + \boldsymbol{u}(\boldsymbol{x}, t) \tag{1}$$

where $\boldsymbol{x}$ and t are space and time coordinates, respectively. The permanent lateral displacements of centrifuge soil models tested using a laminar container are commonly provided by LVDT (Linear Variable Differential Transducer) recordings of motion along the flexible boundaries. Monitoring of permanent displacement within a soil mass is still not practical with currently available sensing devices used in centrifuge testing. Measured displacements along the soil boundaries are sufficient for analyses of permanent deformations in a soil mass only within the context a shear beam model (Elgamal *et al*., 1996) which neglects any variation in motion along the lateral direction. Conversely, the cyclic response is generally monitored using a limited number of vertical arrays of accelerometers located within the soil system as well as at the boundaries (two arrays were employed for the soil systems analyzed below in Sections. 4 and 5). The accelerations recorded by such arrays may be used to estimate the associated displacement field based on global interpolations. Such interpolations determine a single continuous field which is mapped across the whole soil system domain, and may be used to evaluate relatively accurate estimates when a priori information is available on the expected trends.

The cyclic displacement field may be expressed as:

$$\boldsymbol{u}_{\mathrm{c}}(x,t) = \sum_{i-1}^{n} \alpha_i(t)\, \boldsymbol{\Phi}_i(x,t) \tag{2}$$

in which $\boldsymbol{\Phi}_i(\boldsymbol{x}, t)$ are global shape functions, $\alpha_i(t)$ are generalized coordinates, and n is number of shape functions used. The global shape functions are required to satisfy only the system kinematic boundary conditions. A limited number of judiciously selected functions is generally enough to capture the essential characteristics of the cyclic response of soil systems when subjected to an earthquake or similar low frequency excitation. Herein, the functions $\boldsymbol{\Phi}_i$ were selected to be the linear modal configurations of the analyzed systems and were determined using finite element analyses (as described below). Estimation of a displacement field utilizing Eq. (2) is consequently referred to as a spectral motion reconstruction. Within the set of kinematically admissible shape functions, the modal configurations lead to estimates of the displacement field with the least numerical artifacts (i.e., short wave-length terms which are not associated with the observed phenomena). These configurations reflect the system stiffness characteristics, and capture the effects of boundary conditions as well as presence of structural elements or foundation within a soil system. In this study, the mode shapes were also adaptively varied with time to account for any changes in soil stiffness properties during dynamic excitations.

The use of linear modal configurations does not imply an assumed linear or equivalent linear system behavior. These configurations are used only as tools for interpolation and extrapolation.

The non-linearity in a system response is accounted for through the generalized coordinates and the adaptive variation of mode shapes as a function of soil stiffness properties. The time histories of the coordinates $\alpha(t)$ may be evaluated using optimization techniques so that to minimize the discrepancies between recorded and computed cyclic motions. Herein, these coordinates were estimated using a simple least-squares formulation:

$$\min_{\alpha_i(t)} \left(\sum_{s=1}^{m} \| \boldsymbol{u}_{\mathrm{c}}^{(\mathrm{c})}(\boldsymbol{x}_s, t) - \boldsymbol{u}_{\mathrm{c}}^{(\mathrm{r})}(\boldsymbol{x}, t) \| \right) \tag{3}$$

where the index $s = 1,2,\ldots, m$ refers to sensors utilized to monitor the system response, $\boldsymbol{u}_c^{(\mathrm{r})}(\boldsymbol{x}, t)$ is displacement as evaluated through double time integration of accelerations recorded by the sth sensors, and $\boldsymbol{u}_{\mathrm{c}}^{(\mathrm{c})}(\boldsymbol{x}_s, t)$ is corresponding displacement as computed using Eq.(2). The evaluated cyclic displacements using Eqs. (2) and (3) may then be used along with simple differentiation techniques to estimate the associated strain fields.

Accuracy of the spectral motion reconstruction is a function of instrument topology, number of employed shape functions and response characteristics of the analyzed soil system (Appendix I). The maximum number of shape functions which may be used is dictated by number, spacing and configuration of used sensors. A small number of functions is typically required to minimize the generation of interpolation artifacts when using sparse measurements. Conversely, the employed motion records are to be filtered using low-pass windows to reduce the impact of aliasing errors (Bendat and Piersol, 2000) which are associated with the use a limited number of shape functions.

3.2 Time evolution of modal configurations

An eigenvalue problem formulation and the finite element technique (Hughes, 1987) were used to determine the time evolution of the modal configurations of analyzed centrifuge models of saturated soil and soil-pile systems. For a given time widow of observed response with only mild nonlinearities, the equivalent-linear stiffness of the nonlinear system is used to evaluate the corresponding modal configurations. The resultant piecewise time-variation of these configurations reflects any changes in shear and bulk stiffness properties due to a rise in pore fluid pressure or an increase in shear strain amplitudes. The equivalent-linear stiffness properties of the analyzed systems were evaluated based on estimates of corresponding shear wave velocities using

a cross-correlation analysis (Bendat and Piersol, 2000; Elgamal *et al*., 1995). For a centrifuge model excited at the base, this analysis rely on the concept that the cross correlation function $c_{aiaj}(t)$ between lateral accelerations $a_i(t)$ and $a_j(t)$ recorded by sensors i and j located at levels z_i and z_j reaches a major peak at a time delay $t = t_d$, where t_d is average time for dynamic shear waves to travel from i to j (sample results are presented in Sec. 4). Thus, an average shear wave velocity v_s between locations i and j may be estimated as: $v_s = |z_j z_i|/t_d$. The associated equivalent linear shear modulus is then given by $G = \rho v_s^2$ (where ρ is mass density).

The distinctive kinematic boundary conditions imposed by the laminates of the containers used to test the analyzed centrifuge models were idealized using special finite element considerations. These laminates were considered to be infinitely rigid and separated from each other by zero thickness interface elements to idealize the roller bearing contacts (Fig. 1). An elastic-perfectly plastic interface mechanism (having a low elastic stiffness of 10 kPa and a friction coefficient of 0.006) was used to allow the laminates to slide with respect to each other. Note that the modal configurations reflect an equivalent linear behavior, and only the low elastic stiffness of the interface elements has an impact on these configurations.

4 Infinite slope model

The response of actual infinite slopes to lateral base excitations is essentially one-dimensional and may be analyzed accurately using shear beam models. Such slopes are commonly modeled in centrifuge testing using laminar containers to reduce the impact of the side walls and supposedly approach shear beam conditions.

4.1 Centrifuge test

A centrifuge model of an infinite slope consisting of a 6 m soil deposit (Sharp, 1999) was tested at Rensselaer (RPI) under a 30g centrifugal acceleration using a laminar container (Fig. 2). The deposit was composed of a uniform Nevada sand at a relative density D_r of 75% and saturated with a viscous fluid (methocel) to simulate real life permeability (of the order of 4.0 x 10^{-5} m·s^{-1}). The model had a 2° slope which corresponded to a prototype angle of 4.8° after corrections to address the effects of lateral inertia, weight of the rings and water level (Taboada, 1995). A lateral harmonic input excitation having a 2 Hz frequency and amplitude of about 0.2g (prototype units) was applied to the base of the deposit. The soil response was monitored using accelerometers, LVDTs and pore pressure transducers (Fig. 2). The recorded lateral accelerations within the soil deposit and along the boundaries (on the laminates) were marked at shallow depths by significant discrepancies in amplitude and patterns (Fig. 3). As shown below, these discrepancies are associated with a deviation from a shear beam model when a soil deposit experiences significant stiffness degradation associated with a substantial rise in pore pressure or liquefaction.

4.2 Shape functions

Time-evolution of the shear wave velocity profile of the deposit was obtained using cross-correlations (Fig. 4) of overlapping 1s time windows of the recorded accelerations within the soil mass. Four time-phases of distinct velocity profiles were identified, as shown in Fig.5. The observed decrease in velocity with time reflected a significant increase in cyclic shear strain amplitude and rise in pore-fluid pressure. Within the top 2 m soil strata and towards the end of shaking, peak shear strains were as high as 1.5% and pore pressure ratio r_u approached a value of about 1.0 (where r is ratio of excess pore pressure and vertical effective stress), as described below.

A two-dimensional plane strain finite-element model was used to idealize the 6 m single-layer deposit and laminar box of Fig. 2. In addition to the interface elements (Sec. 3.2), the peculiar boundary conditions imposed by the laminar box were accounted for by slaving the displacements of each two elements corresponding to the same laminate (at each of the two lateral sides of the soil deposit). Four sets of mode shapes were evaluated for the laminar container-soil system

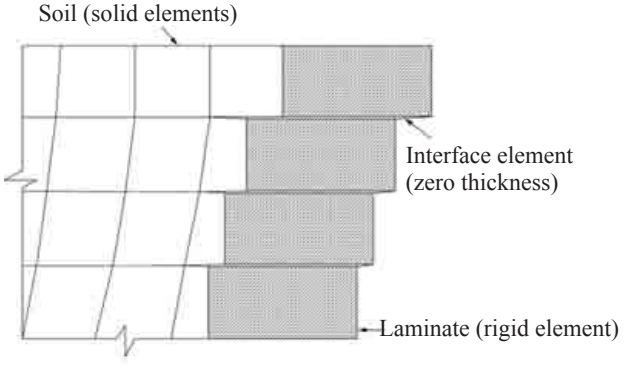

Fig. 1 Schematic details of employed finite element model of soil-laminar container system

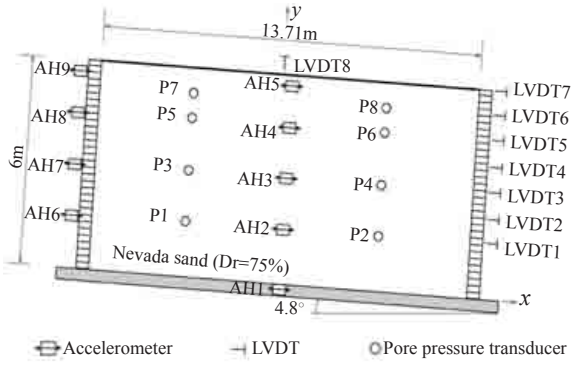

Fig. 2 Configuration of analyzed infinite slope model (Sharp, 1999)

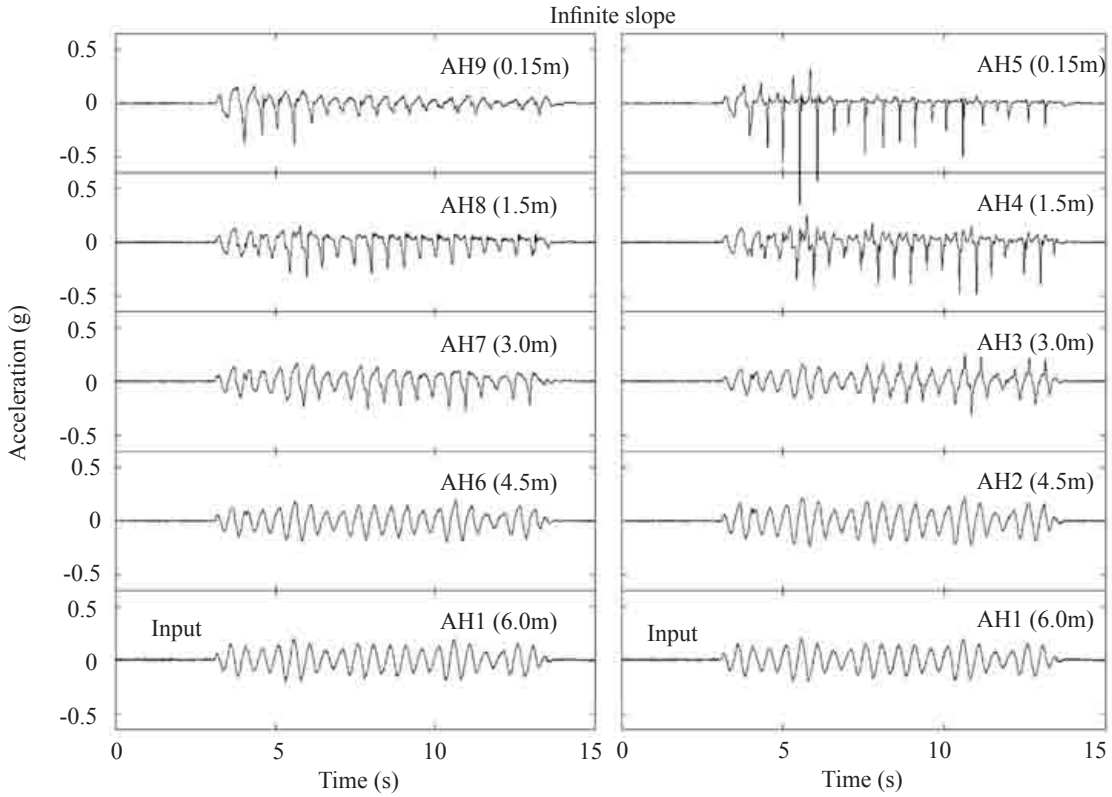

Fig. 3 Acceleration time histories of analyzed infinite slope, as recorded within the soil deposit (AH2 to AH5) and on the laminates (AH6 to AH9)

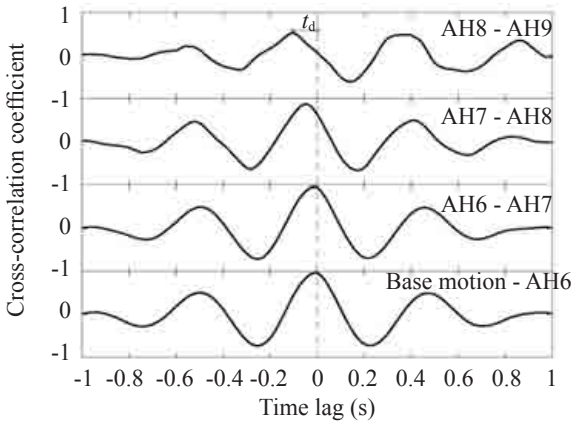

Fig. 4 Cross-correlation of the infinite slope acceleration records for the 4 - 5 s time window

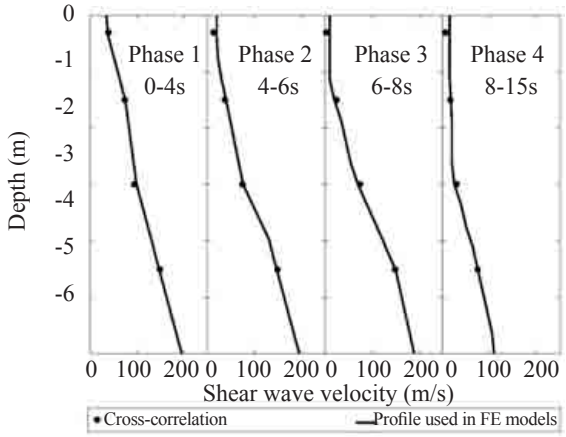

Fig. 5 Time evolution of shear wave velocity profiles of analyzed infinite slope model

using the shear wave velocity profiles of Fig. 5. Figure 6 displays the 1st and 4th sets of modal configurations which were employed in a spectral reconstruction of the infinite slope motion. The contrasting displacement and deformation patterns of these two sets demonstrate the impact of soil softening. For visual clarity, the modal configurations in Fig. 6 were normalized so that the maximum amplitude of displacement is equal to 1 m. In view of the fact that the recorded motion consisted mostly of lateral accelerations and displacements, the employed shape functions were selected to include the first three modal configurations dominated by lateral displacements. A fourth mode which exhibited noticeable vertical displacements was employed to account for the cyclic motion in this direction (as monitored by LVDT8 of Fig. 2)

4.3 Displacement, strain and pore-pressure fields

The four sets of modal configurations mentioned above were employed, along with the recorded motions (provided by accelerometers and LVDTs), to estimate the displacement and strain fields of the analyzed infinite slope. The optimal cyclic displacements evaluated using

Eqs. 2 and 3 and those provided by accelerometer and LVDT recordings were generally in good agreement, as shown in Fig. 7 for selected time instants. Figure 8 displays the lateral normal and shear strain (ε_{xx} and ε_{xy}) fields as well as the distribution of excess pore pressure ratio for the same instants. In this figure, the displacements were amplified 30 times for visual clarity. The pore pressure field was obtained using simple linear 2-D interpolation between measurements provided by the two vertical arrays of pressure sensors shown in

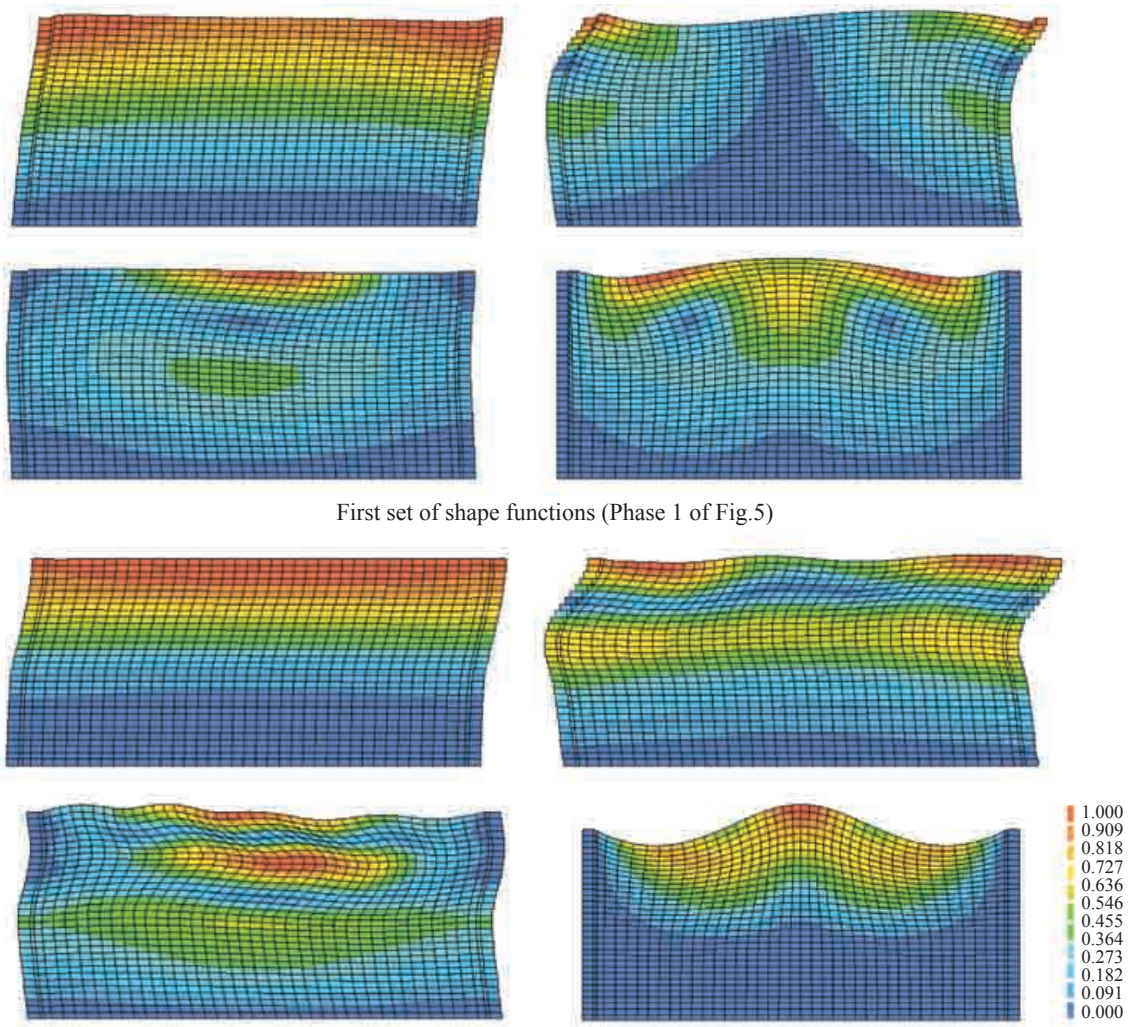

Fig. 6 First and fourth set of shape functions used in analysis of the infinite slope centrifuge model (functions normalized so that maximum displacement amplitude is equal to one, color contours correspond to displacement relative amplitudes)

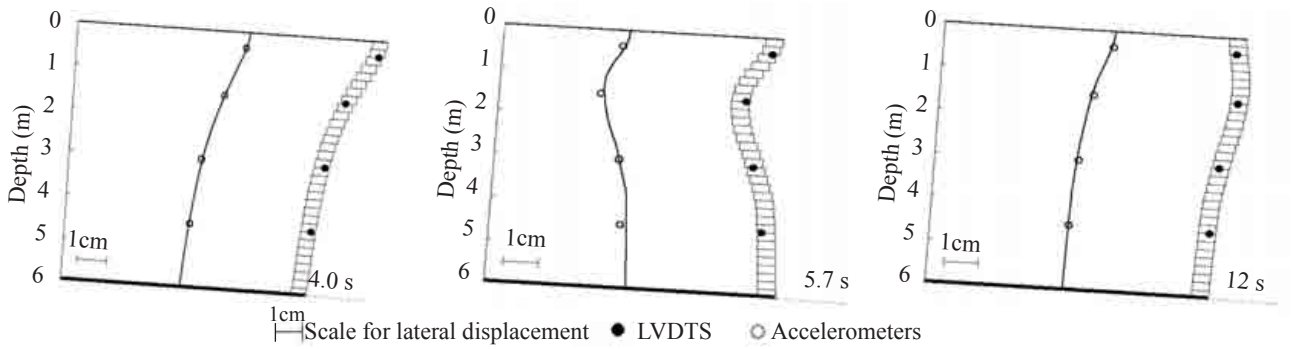

Fig. 7 Measured and estimated lateral cyclic displacements of the infinite slope model (along the AH2-AH5 vertical array and the container laminates) for selected time instants

Fig. 2, along with the appropriate boundary conditions of impermeable base and lateral walls. The entire time histories (visual animation) of these fields are available at RPI (2003).

A zone of high pore pressure ratios with values approaching 1.0 formed within the top 2 m strata after 4 cycles of shaking at about 5 s (areas of light to dark blue in Fig. 8). This zone of liquefied soil did not expand downward in contrast to the response patterns generally exhibited by level sites (Taboada and Dobry, 1993). The pore pressure within the under laying strata increased gradually during the input excitation but did not exceed ratios of the order of 0.75. The visual time-animation of the field of pore-pressure ratios (RPI, 2003) revealed instantaneous decreases in amplitude within these strata. These decreases were associated with a dilative response which occurred at large shear strain amplitudes (reaching values as high as 1.5 %, Fig. 8). The pore fluid-pressure buildup as well as the instantaneous decreases were mostly independent of the lateral direction. A rather marginal evidence of a 2-D response was observed towards the end of shaking within the zone of high pore pressure ratio (i.e., r_u higher than about 0.75, as shown in Fig. 8 for the 12 s time instant).

Relatively large lateral (cyclic) displacements occurred in conjunction with the high pore pressure ratios. These displacements were associated with significant normal lateral strains (ε_{xx}) indicating a deviation of the deposit response from that of a l-D shear beam model when the pore pressure ratio exceeded a value of about 0.75 (Fig. 8). Peak values of these normal strains were as large as 0.15 % near the surface. The corresponding shear strains (ε_{xy}) were non-uniform along the lateral direction (Fig. 8). The large lateral normal strains and deviation from a shear beam response remained confined to the top layers of high pore pressure ratios and accordingly did

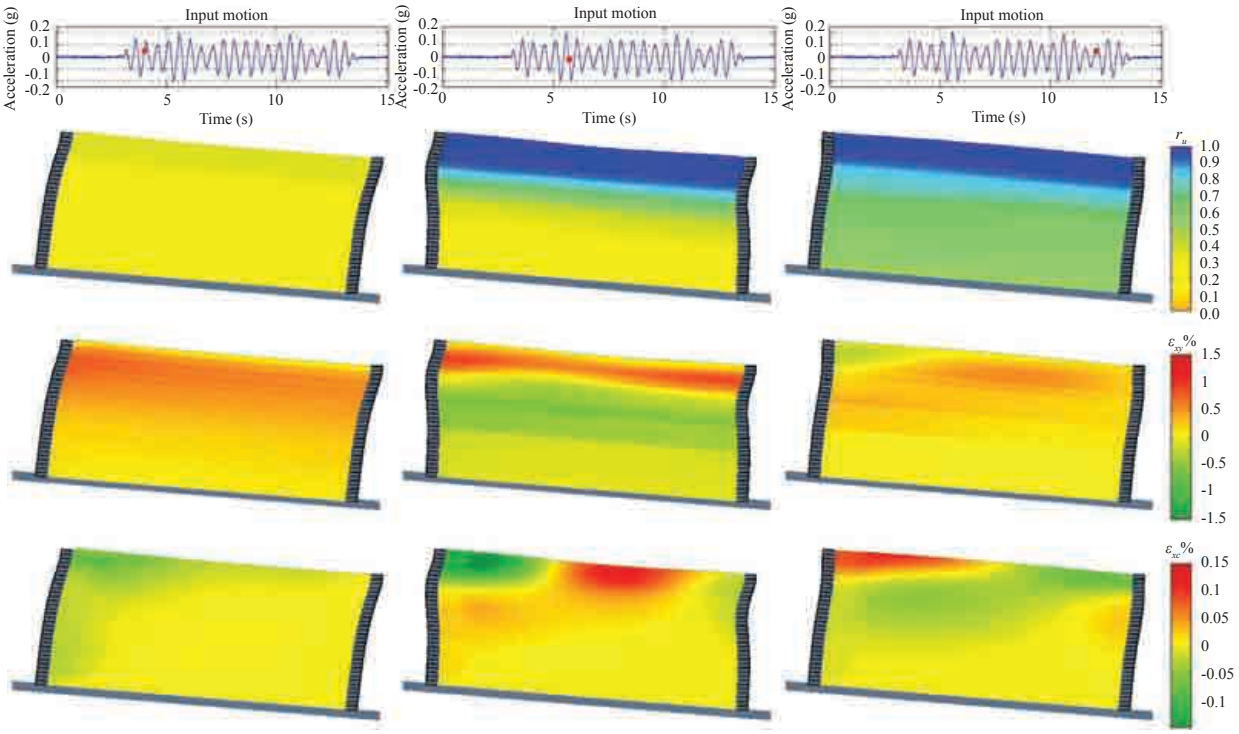

Fig. 8 Pore pressure ratio, shear strain and normal strain fields of the infinite slope model for selected time instants

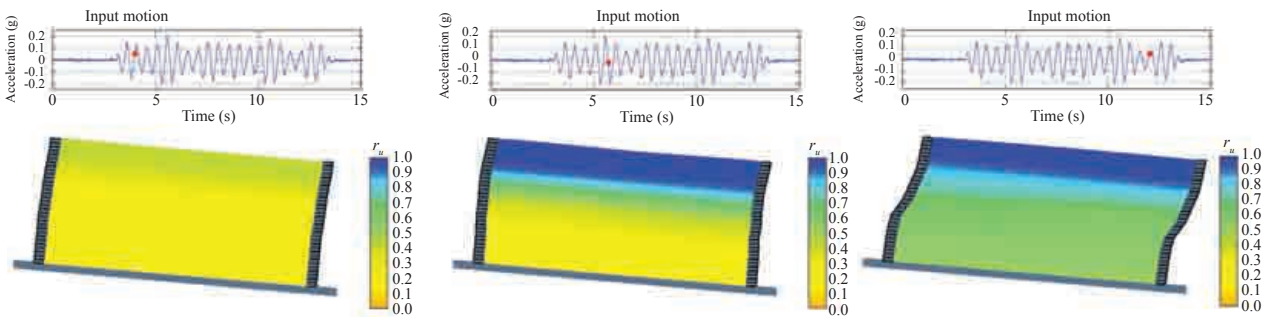

Fig. 9 Permanent displacement profile and pore pressure ratio field of the infinite slope model for selected time instants

not propagate downwards during shaking

The permanent lateral displacements of the analyzed infinite slope were evaluated using the laminate motions recorded by the LVDTs installed along the flexible sides of the employed laminar container (Fig.10). These permanent displacements were assumed to be associated with a shear beam model and linear interpolations were used between LVDT locations to evaluate the associated profiles, as shown along the laminates for selected time instants in Fig. 9 (RPI, 2003). This figure exhibits also the corresponding pore pressure fields. The most significant displacements were found to be limited to the upper soil strata where the pore-pressure ratio, r_u, exceeded a value of about 0.6.

5 Soil-pile model

The response of soil-pile systems to seismic excitations is complex, intrinsically multi-dimensional and a function of stiffness properties of both soil and pile. In centrifuge testing, this response is monitored at selected locations using acceleration, displacement, pore pressure, and strain sensors. Investigation of the response and deformation characteristics of a soil-pile system at discrete (sensor) locations does not provide a full picture of the involved mechanisms. Spectral motion reconstruction was employed herein to analyze the three-dimensional response of a sandy soil-pile centrifuge model.

5.1 Centrifuge test

A centrifuge model of a soil-pile system was tested at RPI (Abdoun, 1997) under a 50 g centrifugal acceleration using a laminar container (Fig.10). The model simulated a free-head single pile embedded in water-saturated sandy deposit and having a diameter of 0.6 m, bending stiffness of EI = 8000 kN·m^2 and height of 8 m (prototype units). The deposit consisted of a 6 m dense (D_r = 85 %) fine Nevada sand layer placed on top of a 2 m thick slightly cemented (non-liquefiable) stratum (Fig. 10). The soil-pile system was inclined 2˚ to the horizontal which corresponded to a 4.8˚ slope after

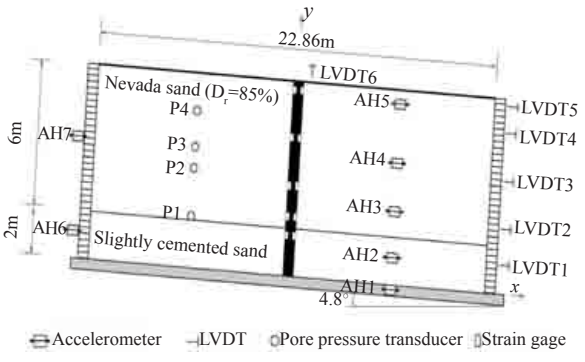

Fig. 10 Configuration of analyzed soil-pile model (Dobry and Abdoun, 2003)

instrumental corrections (Taboada, 1995). The model was subjected to an input excitation consisting of a 40-cycle acceleration parallel to the base of the laminar container and having a uniform amplitude of about 0.3 g and a dominant frequency of 2 Hz. The soil and pile response was monitored in terms of (Fig. 10): (1) lateral accelerations within the soil and on the laminar container, (2) lateral displacements of the container rings, (3) pore-water pressures, and (4) bending strains on pile surface. The measured pile strains were used, along with the Bernoulli's beam theory, to evaluate the corresponding bending moments ($M = EI\ \varepsilon\ /r$, where ε is bending strain measured on pile surface and r is pile radius). The recorded soil lateral accelerations and pile bending moments are shown in Fig. 11.

5.2 Dynamic pile response

The pile moment distribution was evaluated using third order local polynomial interpolations (i.e., soil pressure on the pile was assumed to vary linearly between the strain gage levels shown in Fig. 10), and subsequently employed to estimate the pile lateral displacements. Double integration of the Bernoulli's beam equation of motion gives:

$$u_{\text{pile}}(z) = \int_0^z \left(\int_0^\xi \frac{M(\zeta)}{EI} \mathrm{d}\zeta \right) \mathrm{d}\xi + u_0' z + u_0) \qquad (4)$$

where u_{pile} is pile lateral displacement, M is pile bending moment, ξ and ζ are dummy integration variables of depth, and z is depth coordinate. The constants u'_0 and u_0 were obtained using the following kinematic constraints for the pile, which was considered to be pin-supported at the base and free at the top:

$$u_{\text{pile}}(z = L) = 0, \quad \text{and} \quad u_{\text{pile}}(z = z_p = 0) = u_{\text{soil}}(z = z_p = 0) \qquad (5)$$

here $z = L$ corresponds to the base of the pile, and $z_{p=0}$ is the location where soil exerts a zero pressure on the pile, or p = 0. This location corresponds to an inflection point of the bending moment distribution, or $\partial^2 M(z)/\partial z^2 = 0$

5.3 Shape functions

A three-dimensional finite element model was used to evaluate the modal configurations of the soil-pile-laminar box system (Fig.10). The soil deposit and pile were idealized using solid brick and beam elements, respectively. Cross-correlation analyses of 1s overlapping time windows of the recorded accelerations showed no significant stiffness degradation of the soil during shaking. These analyses provided only averages of the stiffness properties over the employed time windows. Thus, the effects of pore pressure buildup near the soil surface were apparently counterbalanced by a significant dilative response of the dense Nevada sand at large shear strain excursions (as indicated by the

acceleration spikes at the 0.5 m depth, Fig. 11). Note that shorter time windows would lead to a substantial decrease in accuracy of the estimated stiffness averages (Bendat and Piersol, 2000). A single set of seven modal configurations, corresponding to the identified shear wave velocity profile, was used in a spectral motion reconstruction. Figures 12 and 13 display a selection of four shape functions which correspond to low frequency modes.

5.4 Displacement, strain and pore-pressure fields

The cyclic motion of the soil, pile and laminar box were evaluated using the recorded accelerations, displacements and bending strains. The optimal displacements estimated using Eqs. 2-5 and those provided by the sensor measurements are shown in Fig. 14 for selected time instants. As shown clearly in this

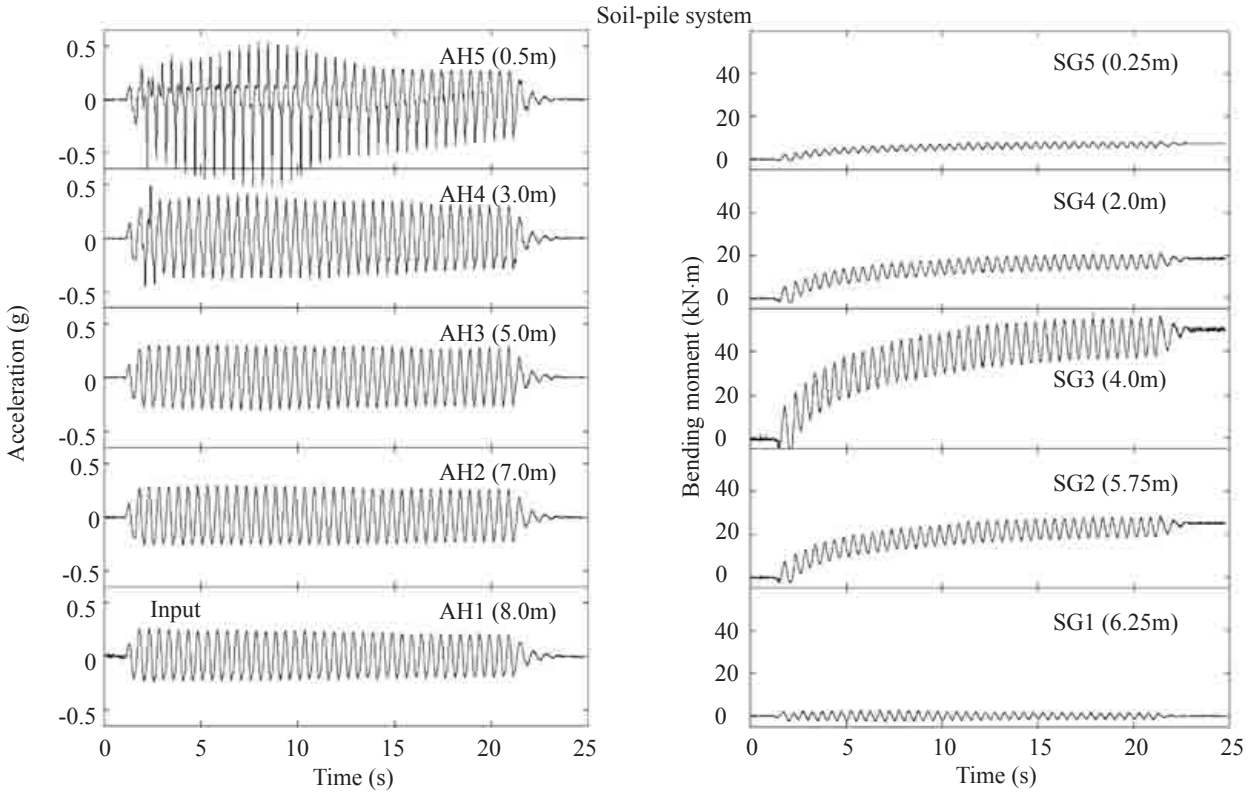

Fig. 11 Acceleration and bending moment time histories of analyzed soil-pile centrifuge model

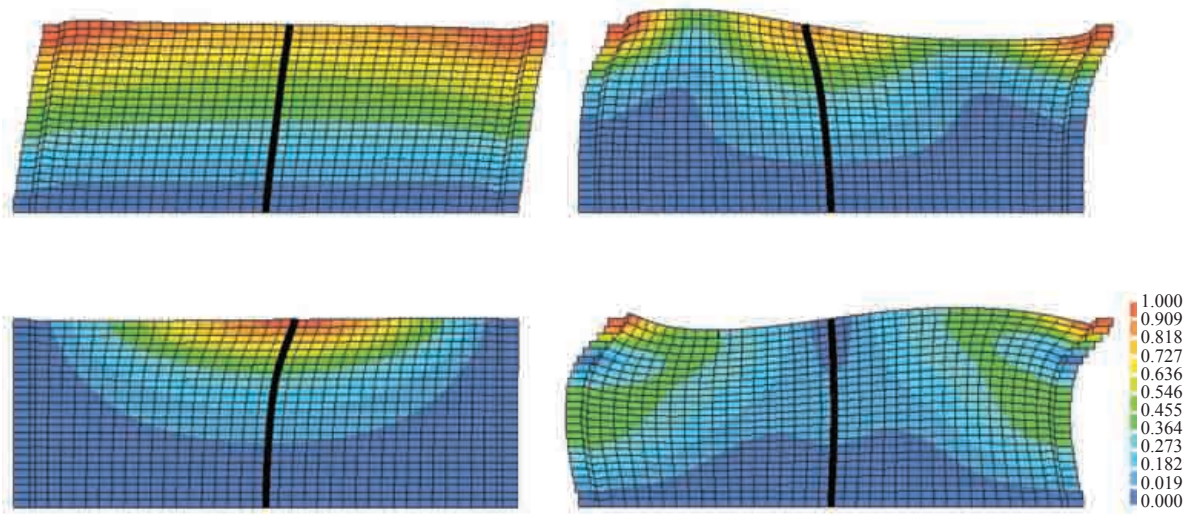

Fig. 12 Cross-sectional view of four 3-D modal configurations out of a set of seven shape functions used in analyses of the soil-pile system of Fig. 10 (color contours correspond to displacement amplitudes)

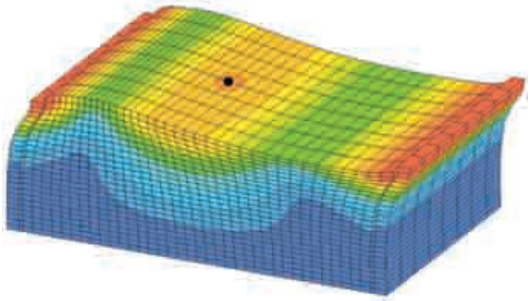

Fig. 13 A 3-D perspective of the second shape function used in analyses of the soil-pile system of Fig. 10 (color contours correspond to displacement amplitudes)

figure, the cyclic motions of pile, soil and laminates were generally out-of-phase in view of non-uniform inertial forces. The displacement and strain fields along the central longitudinal cross-section of the soil-pile-laminar box system are displayed in Fig. 15 for the same instants. For visual clarity, these displacements were amplified 20 times. Figure 15 also exhibits the excess pore pressure profile along the vertical array P1-P4 of Fig. 10 (the pore pressure multidimensional distribution could not be approximated using the measurements of a single vertical array). The entire time histories (visual animation) of these fields are available at RPI (2003).

The top 2 m of soil strata liquefied after 5 cycles of shaking (at about 3.5 s) as the excess pore pressure ratio reached values higher than 0.9 (Fig. 15). This high ratio

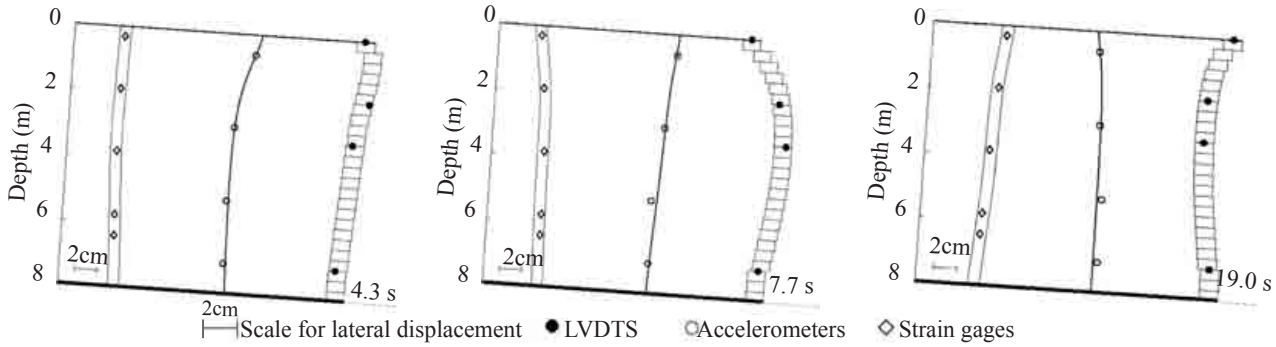

Fig. 14 Measured and estimated cyclic displacements of the soil-pile model for selected time instants

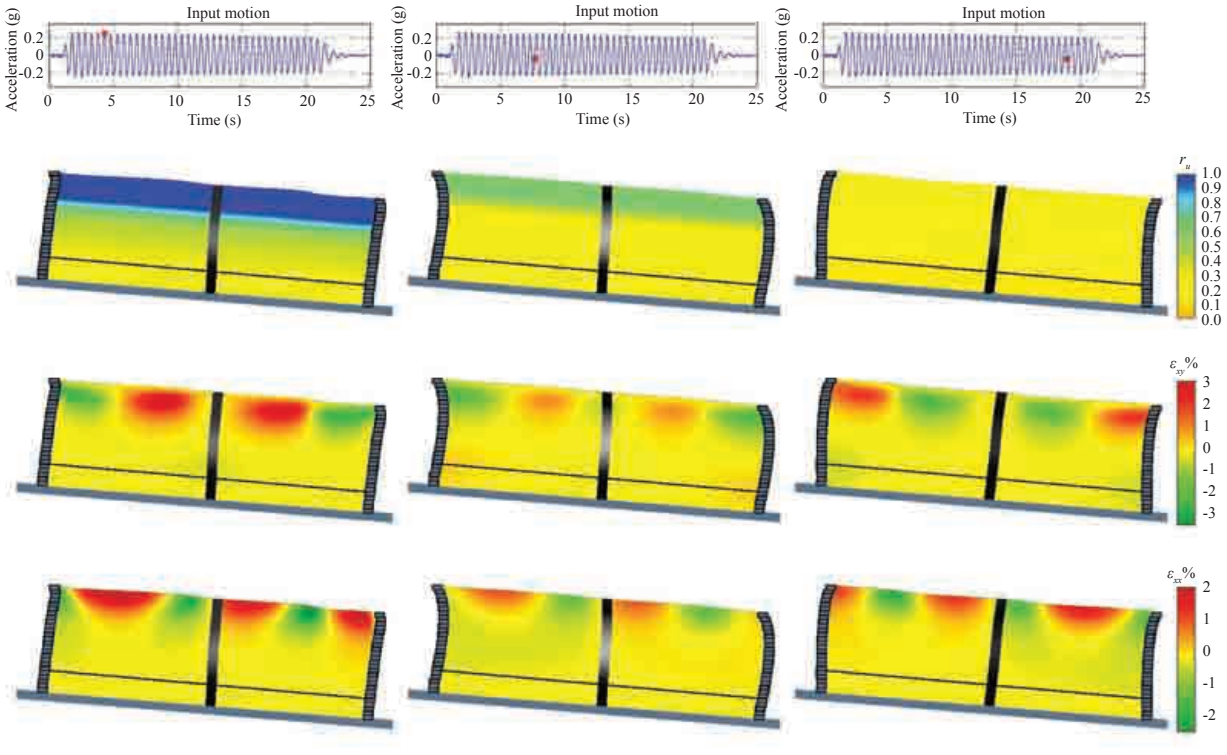

Fig. 15 Pore pressure ratio, shear strain and normal strain fields of the soil-pile model for selected time instants

was sustained for 15 cycles (i.e., 7.5 s) of shaking. The visual time-animation of the associated profiles [20] revealed instantaneous decreases in excess pore pressure amplitude during this time window within the top 2 m strata. These decreases were associated with a dilative response at large shear strain amplitudes. Indeed, large lateral cyclic displacements and strains developed within the liquefied zone as indicated by areas of dark green and red colors in Fig. 15. After an initial transition phase, the lateral shear strain (ε_{xy}) waves were of a standing nature, rather than traveling, and reached a peak value of about 3.5 % near the ground surface.

The lateral normal strains (ε_{xx}) approached values of the order of 2.5 % as the soil mass interacted with the pile and walls of the laminar box. The pore water pressure buildup dissipated gradually during the second-half of input excitation (i.e., the last 20 cycles of shaking). Nevertheless, the shear and normal strains remained large in the shallow zones near the deposit free surface.

The magnitude of bending strains of the pile is depicted in Fig. 15 by shades of gray (lighter shades correspond to larger strains and bending moments). The maximum bending strains developed below the interface between liquefied and non-liquefied soil strata, and well above the cemented base layer. These findings are consistent with results of centrifuge tests and observations made by Dobry *et al*. (2003).

6 Conclusions

A simple identification technique was developed to visualize and analyze the mechanisms of deformation and pore-pressure buildup of centrifuge models of saturated soil and soil-structure systems subjected to dynamic excitations. Optimal time histories of displacement and strain fields were estimated from spatially-sparse acceleration and displacement records based a spectral motion reconstruction expressed in terms of modal configurations. These configurations were adaptively varied in time in order to account for soil stiffness reduction with shear strain amplitude and degradation with pore pressure buildup. Visualization of the free- and near-field dynamic response of infinite slope and soil-pile systems revealed salient multi-dimensional deformation patterns, especially within zones of high pore pressure ratios. Significant normal strains were found to develop within liquefied soil strata of the analyzed free-field infinite slope and the response was shown to deviate from a shear beam idealization. The spectral motion reconstruction technique provides an effective tool to visualize the dynamic response of centrifuge, shake-table and field soil systems.

Acknowledgments

This research was supported by the National Science Foundation, Grant No. CMS-9984754. This support is gratefully acknowledged.

References

Abdoun T (1997), "Modeling of Seismically Induced Lateral Spreading of Multi-layer Soil Deposits and Its Effects on Pile Foundations," *Ph.D. thesis*, Rensselaer Polytechnic Institute, Troy, NY.

Bendat JS and Piersol AG (2000), *Random Data: Analysis and Measurement Procedures*, John Wiley and Sons.

Brodlie K and Mashwama P (1997), *Controlled Interpolation for Scientific Visualization*, IEEE Computer Society, Chap. 11 from Scientific Visualization: Overviews, Methodologies, Techniques by G.M. Nielson, H. Hagen and H. Muller.

Dobry R and Abdoun T (1998), "Post-triggering Response of Liquefied Sand in the Free-field and Near Foundations," *Proc. of ASCE Specialty Conf. on Geotech, Earthquake Engrg. and Soil Dyn*., Vol.1: 270-300, Seattle, WA, ASCE.

Dobry R and Abdoun T (2001), "Recent Studies on Seismic Centrifuge Modeling of Liquefaction and Its Effect on Deep Foundations," S. Prakash, *Proc. 4th Intl. Conf. on Rec. Adv. in Geotech, Earthquake Engrg and Soil Dyn*. -Symposium to Honor Prof W.D.L. Finn, pages SOAP- 3, San Diego, CA.

Dobry R, Abdoun T, O'Rourke TD and Goh SH (2003), "Piles in Lateral Spreading: Field Bending Moment Evaluation," *Journal of Geotechnical and Geoenvironmental Engineering*, ASCE, **129** (10):879-889.

EERI (2004), "Securing Society Against Catastrophic Losses: A Research and Outreach Plan in Earthquake Engineering,"*Technical Report*, Earthquake Engineering Research Institute.

Elgamal A, Lai T, Yang Z and He L (2001), "Dynamic Soil Properties, Seismic Downhole Arrays and Applications in Practice," *Proc. 4th Inti. Conf. on Rec. Adv. in Geotech*, *Earthquake Engrg and Soil Dyn*., pages SOAP-6, San Diego, CA.

Elgamal AW, Zeghal M, Dobry R and Taboada VM (1996), "Analysis of Site Liquefaction and Lateral Spreading Using Centrifuge Testing Records," *Soils and Foundations*, **36**(2): 111-121.

Elgamal WA, Zeghal M, Tang T and Stepp C (1995), "J. Lotung Downhole Array I: Evaluation of Site Dynamic Properties," *J. of Geotec. Engrg.*, **121**(4):350-362.

Hamada M, Isoyama R and Wakamatsu K(1996), "Liquefaction-induced Ground Displacement and Its Related Damage to Lifeline Facilities," *Soils and Foundations,* Special Issue on Geotechnical Aspects of the January 17, 1995 Hyogo-Ken Nambu Earthquake, pp.81-97.

Hughes TJR (1987), *The Finite Element Method: Linear Static and Dynamic Finite Element Analysis*, Prentice-Hall, Englewood Cliffs, NJ.

Kallou PV (2002), "Visualization Analysis of the Dynamic Response of Soil and Soil-pile Systems," *Master's thesis*, Rensselaer Polytechnic Institute, Troy, NY.

NRC (1985), "Liquefaction of Soils during Earthquakes," *Rept. No. CETS-EE-001*, Committee on Earthquake Engineering, National Research Council, Washington, DC.

Perke E (1995), *Animation and the Examination of Behavior over Time,* Chap. 7 from Computer Visualization: Graphics Techniques for Scientific and Engineering Analysis, edited by R. S. Gallagher, H. Hagen and H. Muller, CRC Press.

RPI (2003), "Visualization of Soil and Soil-structure Response in the Presence of Liquefaction," Geotechnical Centrifuge Research Center, www.nees.rpi.edu/research/visualization.shtml, Rensselaer Polytechnic Institute.

Sharp KM (1999), "Development of Prediction Charts for Liquefaction Induced Lateral Spreading from CPT Tests," *Ph.D. thesis*, Rensselaer Polytechnic Institute, Troy, NY.

Taboada V (1995), "Centrifuge Modeling of Earthquake-Induced Lateral Spreading Using a Laminar Box," *Ph.D. thesis*, Rensselaer Polytechnic Institute, Troy, NY.

Taboada V and Dobry R (1993), "Experimental Results of Model No.l at RPI," K. Arulanandan and R. Scott, *International Conference on the Verification of Numerical Procedures for the Analysis of Soil Liquefaction Problems (VELACS)*, 1: 3-17, Davis, California, Balkema, Rotterdam.

Tokimatsu K (1999), "Performance of Pile Foundations in Laterally Spreading Soils," Seco e Pinto, *2nd Intl. Conf. on Earthquake Geotech*. Engrg, **3**: 957-964. Balkema, Rotterdam.

Van Laak P, Taboada V, Dobry R, and Elgamal AW (1994), "Earthquake Centrifuge Modeling Using a Laminar Box," Drnevich V. P. Ebelhar, R. J. and B. L. Kutter, *Dynamic Geotechnical Testing*, ASTM STP 1213, volume II. American Society of Testing Materials, Philadelphia.

Vukazich SM and Mish KD (1994), "Using Animation Tools to Evaluate the Quality of Nonlinear Modal Analyses," *Proc. of the NSF Workshop on Visualization Application in Earthquake Engineering*, California State University, Chico, pp.1-7.

Zeghal M, Elgamal W, Tang AT and Stepp C (1995), "J. Lotung Downhole Array II: Evaluation of Soil Nonlinear Properties," *J. of Geotech. Engrg*., **121**(4): 363-378.

Appendix: Analysis Accuracy

Accuracy of the displacement and strain fields evaluated using the spectral motion reconstruction technique is a function of: (1) instrument topology and quality of measurement data, (2) characteristics of monitored response, and (3) correctness of employed modal configurations.

The topology and distribution of measurements dictate the number of modal configurations that may be used in a spectral motion reconstruction. In turn the used modal configurations will prescribe the highest response frequency that may be estimated with a reasonably accuracy. In general, the number of modal configurations should be significantly lower than that of the sensors used in order to reduce and eventually eliminate the generation of spurious spatial oscillations that are nothing but artifacts. Correctness of the employed modal configurations is contingent on realistic estimates of the evolution of stiffness properties in space and time. Shear wave velocities evaluated using cross-correlation analyses of recorded accelerations (as described above) provide only spatial averages of stiffness properties between acceleration locations. The associated modal configurations may not be used in spectral motion reconstruction to capture abrupt changes or localized deformations patterns, such as those related to shear bands or water interlayers. The analyzed centrifuge models consisted of very dense sand (D = 75% and 85%), which ensured that no significant localized phenomena developed during shaking.

The estimated lateral displacement and strain field in this study were relatively accurate in view of the 2 Hz harmonic input excitation and the limited frequency bandwidth of the response of these models. However, the cyclic and permanent settlements of the analyzed soil systems were recorded at a single location (on the free surface, Figs. 2 and 10). The shape functions used in spectral interpolations were therefore selected to consist mostly of modal configurations dominated by lateral displacements. The accuracy of the estimated cyclic settlements is consequently expected to be lower than that of the displacements in the lateral direction.